PSFC/RR-02-10

Multi-Machine Global Confinement and H-mode Threshold Analysis

Working Group*

October 2002

Plasma Science and Fusion Center
Massachusetts Institute of Technology
Cambridge, MA 02139 USA

*Alcator C-Mod: J.A. Snipes, M. Greenwald; ASDEX/ASDEX Upgrade: F. Ryter, O.J.W.F. Kardaun, J. Stober; COMPASS-D/ START/MAST: M. Valovic, S.J. Fielding, A.Sykes, A. Dnestrovskij, M. Walsh; DIII-D: J.C. DeBoo, T.N. Carlstrom; FTU: G. Bracco; JET/ EFDA: E. Righi, R. Sartori, J.G. Cordey, K. Thomsen, D. McDonald; JFT-2M/ JT-60U: Y. Miura, T. Takizuka, T. Fukuda, Y. Kamada, K. Shinohara, K. Tsuzuki, H. Urano; PBX-M/PDX/ TFTR/NSTX: S.M. Kaye, C. Bush; TCV: Y. Martin; TdeV: A. Cote, G. Pacher; TEXTOR: J. Ongena; TUMAN-3M: S. Lebedev; T-10: V. Leonov, A. Chudnovskiy.

This work was supported by the U.S. Department of Energy, Cooperative Grant No. DE-FC02-99ER54512. Reproduction, translation, publication, use and disposal, in whole or in part, by or for the United States government is permitted.

Multi-Machine Global Confinement and H-mode Threshold Analysis

ITPA Confinement and H-mode Threshold Database Working Group[#] presented by J. A. Snipes[*]

[#]From Alcator C-Mod: J.A. Snipes, M. Greenwald; ASDEX/ASDEX Upgrade: F. Ryter, O.J.W.F. Kardaun, J. Stober; COMPASS-D/ START/MAST: M. Valovic, S.J. Fielding, A. Sykes, A. Dnestrovskij, M. Walsh; DIII-D: J.C. DeBoo, T.N. Carlstrom; FTU: G. Bracco; JET/ EFDA: E. Righi, R. Sartori, J.G. Cordey, K. Thomsen, D. McDonald; JFT-2M/ JT-60U: Y. Miura, T. Takizuka, T. Fukuda, Y. Kamada, K. Shinohara, K. Tsuzuki, H. Urano; PBX-M/ PDX/ TFTR/NSTX: S.M. Kaye, C. Bush; TCV: Y. Martin; TdeV: A. Cote, G. Pacher; TEXTOR: J. Ongena; TUMAN-3M: S. Lebedev; T-10: V. Leonov, A. Chudnovskiy.

[*]MIT Plasma Science and Fusion Center, Cambridge, MA 02139 USA.
e-mail contact of main author: snipes@psfc.mit.edu

Abstract. The ITPA Confinement and H-mode Threshold Databases have been used to analyze energy confinement at high density and the dependencies of the H-mode threshold power on aspect ratio ($R/a = 1/\varepsilon$), edge safety factor, and plasma effective charge (Z_{eff}). High density data from ASDEX-Upgrade, DIII-D, and JET indicate that with peaked density profiles it is possible to maintain good global energy confinement (H98y2 ~ 1) up to and beyond the Greenwald density limit even though the loss power ($P_L = P_{OH} + P_{aux}^{abs} - dW/dt$) does not exceed the H-mode threshold power scaling. The new low aspect ratio MAST data in the threshold database permits initial regressions to be made including the aspect ratio. The inverse aspect ratio dependence of the threshold power cannot be determined with the present dataset due to inconsistencies in the threshold between low inverse aspect ratio devices (ASDEX, PBX-M) and MAST. New scalings for the threshold power have been produced, which yield similar values as previous scalings for the predicted threshold power in ITER. There is an increase in the H-mode threshold at low $q_{95} < 3$ found in ASDEX-Upgrade, COMPASS, DIII-D, JFT-2M, JT-60U, TCV, and TUMAN-3M. The strong increase in the threshold power at low density is also correlated with increased Z_{eff}.

1. Introduction

The ITPA Confinement [1] and H-mode Threshold [2] Database Working Groups analyze global parameters from a number of tokamaks worldwide to better understand the physics of energy confinement in a tokamak and of the transition between L and H-mode. Another aim of the work is to improve confinement and threshold predictions for future devices. In the confinement area, high density data from DIII-D, ASDEX-Upgrade, and JET approaching or exceeding the Greenwald density limit have been added to the database allowing improved analysis of confinement at high density. In the threshold area, new data from Alcator C-Mod include an inner gap scan as well as corrections to the absorbed ICRF power. New threshold data from ASDEX Upgrade in the new divertor DIVIIb, allowing well baffled operation at higher triangularity, have been added to the database. This dataset includes 58 threshold points with NBI and ICRF and variations of B_T, I_p and density. A particular feature of this contribution is that it also includes a variation in triangularity up to 0.35 compared to the previous maximum value of only 0.15. These points suggest an increase of the power threshold with triangularity. New initial ohmically heated H-mode threshold results in double null deuterium plasmas with inboard gas puffing from the low aspect ratio spherical tokamak MAST have also been included in the database. The double null configuration was chosen because it has a lower threshold than single null for these conditions [3]. The inboard gas puffing was shown to lower the threshold in COMPASS-D [4] and this effect also takes place in MAST [5]. Data were taken from a density scan at fixed toroidal magnetic field, $B_T \approx 0.4$T

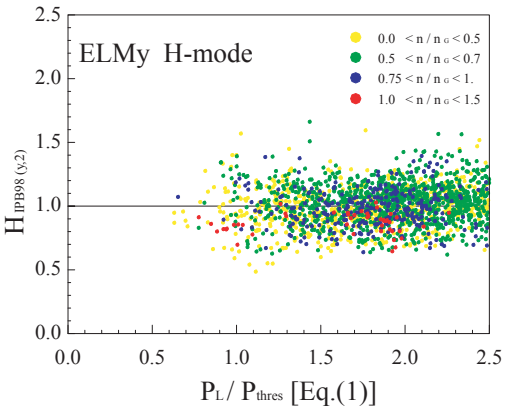

Fig. 1. IPB98(y,2) H-factor vs P_L/P_{thr} from the H-mode Confinement Database with the latest H-mode threshold power scaling from Eq. 1.

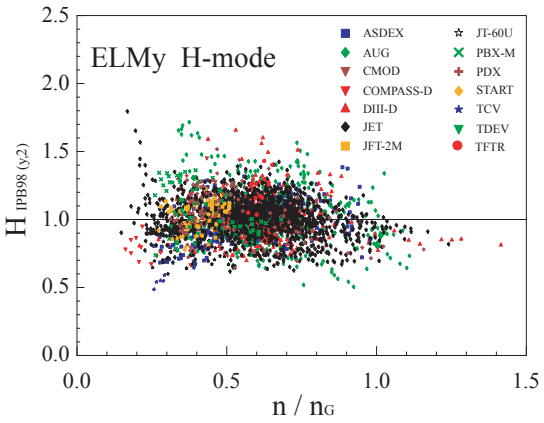

Fig. 2. IPB98(y,2) H-factor vs n/n_G from the H-mode Confinement Database.

(vacuum field at magnetic axis), plasma current $I_p \approx 0.6$MA, major radius R≈0.75m, minor radius a≈0.52m (ε_{MAST}=a/R=0.68) and elongation $\kappa \approx 1.9$. There are also new data from TCV at higher safety factor ($q_{95} > 2.5$), which have a lower threshold. H-mode threshold data from the small circular tokamak TUMAN-3M in Russia have also been included in the database.

2. Confinement Analyses

The high density data from ASDEX-Upgrade, DIII-D, and JET indicate that, under some conditions with peaked density profiles, it is possible to maintain good global energy confinement (H98y2 ~ 1) up to and beyond the Greenwald density limit even when the loss power ($P_L = P_{OH} + P_{aux}^{abs} - dW/dt$) is near the H-mode threshold power scaling ($P_{thres} = 1.67 \cdot \bar{n}_e^{0.61} B_T^{0.78} a^{0.89} R^{0.94}$). Of possible interest to next step devices, a number of machines find that good energy confinement relative to the standard H-mode scaling [1] (IPB98(y,2) ~ 1) can be obtained in H-mode down to a ratio of $P_L/P_{thr} < 1$ (Figure 1). These data suggest that good confinement can be obtained in H-mode even when the loss power is only just above the threshold power scaling at H-mode densities. An estimate of the power necessary to ensure good H-mode confinement is then the H-mode threshold power scaling evaluated at the desired steady-state H-mode density.

Figure 2 shows the H-mode energy confinement scaling IPB98(y,2) versus n/n_G, where n_G (10^{20} m^{-3}) = I_p(MA)/(πa^2) is the Greenwald density limit [6]. While most of the database lies between $0.3 < n/n_G < 0.8$, a number of points from ASDEX-Upgrade, DIII-D, and JET reach and even exceed $n/n_G = 1$ while maintaining good energy confinement, though there is a weak degradation at very high values. In the highest density cases, densities up to 40% above the Greenwald limit were reproducibly achieved in high confinement, ELMing H-mode discharges in DIII-D [7]. Simultaneous gas fueling and good divertor pumping were important to achieving these results. Spontaneous peaking of the density profile was also important as without this profile peaking the energy confinement at high density degraded due to a reduced H-mode pedestal pressure associated with closely coupled core and pedestal temperatures observed at high density [8]. The IPB98(y,2) H-factor also shows a weak increase with density peaking factor ($\gamma_n = 0.5 \cdot (n_{e0}/\bar{n}_e + \bar{n}_e/\langle n_e \rangle)$) [9]. The regression fit to

the residuals for these two effects is H98(y,2) = (1 – 0.07 n/n_G + 0.17 γ_n), showing that they have small influences on the overall H-factor, however, for interaction between shaping and n/n_G, refer to Kardaun [10].

Experimentally observed confinement times for L- and H-mode discharges in T-10 are in good agreement with the predictions of both the L-mode [11] and the IPB98(y,2) H-mode scalings. It may be a result of the crossing of these scalings at high aspect ratios A ~ 5, which is the same as the T-10 tokamak, but may also be an effect of normalized magnetic field related to inverse ρ_* [9,12].

3. Threshold Analyses

The new data added to the threshold database warrant new regressions to better determine a predictive scaling for the threshold power in future devices. In particular, the higher q_{95} data from TCV with lower thresholds have brought its data in line with many of the other tokamaks. The new low aspect ratio MAST data now extend the range of inverse aspect ratio in the database to $0.16 < \varepsilon < 0.69$, which should permit initial regressions to be made including the inverse aspect ratio. However, the dependence of the threshold on inverse aspect ratio is not consistent across the various tokamaks. In particular, PBX-M and ASDEX have the lowest ε, with high and low elongation, respectively. MAST has the highest ε and has high elongation, yet all three of these devices lie well above the threshold scalings without ε and κ. This would imply that the threshold power increases at both low ε and high ε and/or at both low κ and high κ. The initial MAST results are also in a double null configuration where for conventional aspect ratio tokamaks the H-mode threshold is often considerably higher than in single null. When regressions are performed including PBX-M and ASDEX but not MAST, a weak negative dependence of the threshold on ε is found. When PBX-M and ASDEX are excluded but MAST is included, a weak positive dependence of the threshold on ε is found. Due to these inconsistencies in the data from these machines, it is not possible with the present database to determine a reliable scaling of the threshold power including the inverse aspect ratio dependence with all of these devices.

To compare with the previous work on the H-mode threshold scalings from this database group [2], new regressions have been performed on the 9 tokamaks that satisfy the standard low threshold criteria including deuterium plasmas with a single null with the ion ∇B drift toward the X point (excluding PBXM, MAST and TUMAN-3M). In the previous work, all low density points with $\bar{n}_e < 2.2 \times 10^{19}$ m^{-3} were excluded because they tended to have higher thresholds. Now, this low density limit has been adjusted for each machine. The new fits for these 9 tokamaks are (660 points):

$$P_{thres} = 1.67 \pm 0.30 \cdot \bar{n}_e^{0.61\pm0.07} B_T^{0.78\pm0.06} a^{0.89\pm0.13} R^{0.94\pm0.18} \qquad \text{RMSE} = 25.1\% \quad (1)$$

$$P_{thres} = 0.050 \pm 0.005 \cdot \bar{n}_e^{0.46\pm0.06} B_T^{0.87\pm0.06} S^{0.84\pm0.03} \qquad \text{RMSE} = 26.0\% \quad (2)$$

where the standard regression variables of line averaged density and toroidal field are used together with either the major and minor radii or a formula for the surface area of the plasma, $S = 4\pi^2 aR((1+\kappa^2)/2)^{0.5}$. The units here and throughout the rest of the paper are MW, 10^{20} m^{-3}, T, lengths in m. The root mean square errors of these fits are about 1% lower than those of the previous work and the toroidal field dependence has increased, the density dependence has decreased, and the size dependence is nearly the same as before. Figure 3 shows the fit to Eq. 2 and the PBXM, MAST, and TUMAN-3M data have also been plotted for comparison.

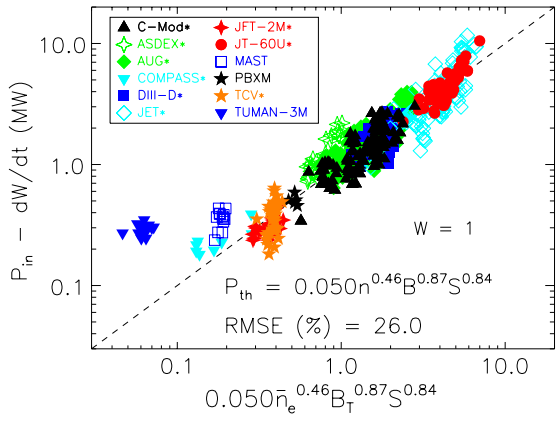

Fig. 3. Measured H-mode threshold power vs. a regression fit to the data from nine tokamaks (with asterisks) given by Eq. 2.

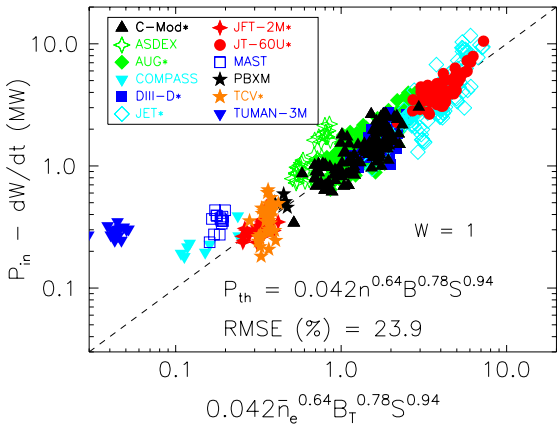

Fig. 4. Measured H-mode threshold power vs. a regression fit to the data from seven tokamaks (with asterisks) given by Eq. 3.

In the previous work, tokamaks with particularly large discrepancies from the standard regression fits were excluded to attempt to make a more homogeneous dataset and reduce the overall RMSE to attempt to improve the accuracy of the H-mode threshold power prediction for next step devices. In that case, six tokamaks (Alcator C-Mod, ASDEX Upgrade, DIII-D, JET, JFT-2M, and JT-60U) were used that all fell close to the standard scalings. Now that lower threshold, higher $q_{95} > 2.5$ data have been included in the database from TCV, those data now also fit reasonably well the standard scalings. So, a fit has now been performed on these 7 tokamaks (615 points):

$$P_{thres} = 0.042 \pm 0.004 \cdot \bar{n}_e^{0.64\pm0.06} B_T^{0.78\pm0.06} S^{0.94\pm0.04} \qquad \text{RMSE} = 23.9\% \qquad (3)$$

which has almost 1% higher RMSE than the 6 tokamak equivalent scaling from the previous work because of the increased scatter in the TCV data. This result has lower density and lower size dependence and higher toroidal field dependence than previously. Figure 4 shows the fit to Eq. 3 with the other 5 tokamaks also plotted on the graph for comparison.

It has long been observed in a number of tokamaks that the H-mode threshold increases at low edge safety factor. Figure 5 shows data from all of the tokamaks in the threshold database comparing the ratio of the measured threshold power to that of Eq. 3 versus q_{95}, where $q_{cyl} = 5\ a^2\ B_T/(R\ I_p)$ (with I_p in MA) is used for the circular tokamak TUMAN-3M. This data includes the standard selection for the threshold as well as high threshold data below the low q limit for each device. Clear increases in the threshold power are observed in a number of tokamaks for $q_{95} < 3$. There are, however, a number of low threshold points from JET between $2.5 < q_{95} < 3$. Since the edge shear also depends sensitively on q_{95}, this may indicate that the stability of edge turbulence plays a role in determining the H-mode threshold. However, edge shear and other stability properties are not available in the threshold database to further check this hypothesis.

To examine the effect of Z_{eff} on the threshold, we include low density data where the threshold is higher than the standard selection data used in the regressions. Although there is a limited dataset in the database with valid Z_{eff} values, Z_{eff} increases with decreasing density, so that the highest thresholds relative to the scaling tend to also be at low density. Figure 6 shows a strong correlation between Z_{eff} and the measured H-mode threshold power normalized to the threshold scaling given by Eq. 3 from the five tokamaks in the database with valid Z_{eff} values. Using Z_{eff} rather than density has the advantage of putting all of the

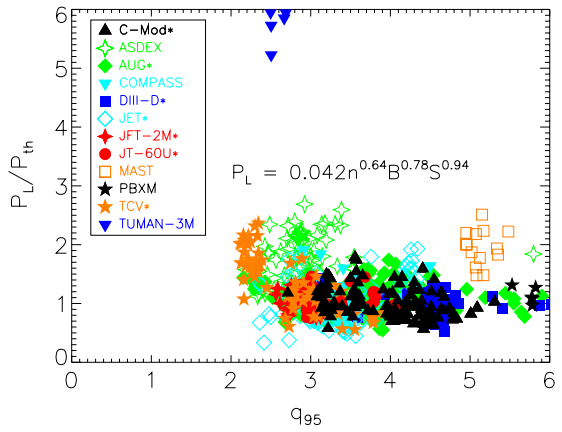

Fig. 5. Measured H-mode threshold power normalized to that of Eq. 3 vs. q_{95} showing a trend to increase the relative threshold power for $q_{95} < 3$.

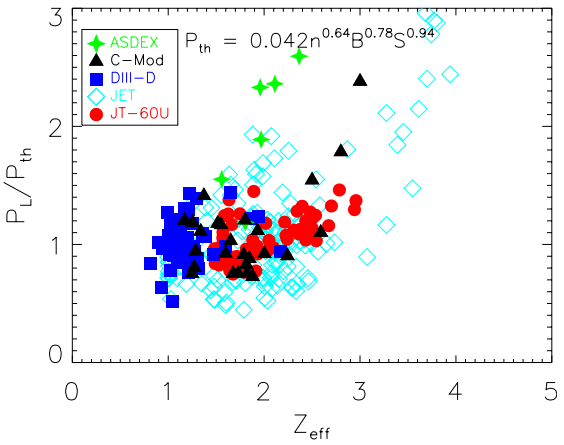

Fig. 6. Measured H-mode threshold power normalized to that of Eq. 3 vs. Z_{eff} showing that the relative threshold power increases strongly with Z_{eff}.

tokamaks on a common scale. There is a clear increase in the relative threshold power with increasing Z_{eff}. This suggests that the low density limit for obtaining the H-mode is strongly correlated with increasing Z_{eff} at low density.

4. Conclusions

Under some conditions with peaked density profiles, it is possible to achieve H factors IPB98(y,2) ~ 1 up to and beyond the Greenwald density limit and it is possible to achieve this level of energy confinement at a power level given by the H-mode threshold scaling (Eq. 1) evaluated at the full H-mode density. The latest prediction from 7 tokamaks with ITER similar configurations (Eq. 3) for the threshold power required in deuterium plasmas in ITER at $\bar{n}_e = 5 \times 10^{19}$ m^{-3} and $B_T = 5.3$ T is 44 MW, with a 2 standard deviation uncertainty interval of 28 to 71 MW. This is somewhat lower than the previous 6 tokamak scaling [2], which gave a point prediction of 52 MW and a 2 standard deviation uncertainty interval of 34 – 80 MW because of the additional TCV data. Similarly, the predicted thresholds in FIRE (at $\bar{n}_e = 2.4 \times 10^{20}$ m^{-3}, $B_T = 10$ T) and Ignitor (at $\bar{n}_e = 3.25 \times 10^{20}$ m^{-3}, $B_T = 12$ T) are 24 MW and 17 MW, respectively. Low $q_{95} < 3$ and high Zeff > 2 also lead to higher threshold power.

References

[1] ITER-Physics-Expert-Groups, *Nuclear Fusion* **39** (1999) 2175.
[2] F. Ryter and the H-mode Threshold Database Group, *Plasma Phys Contr Fus* **44** (2002) A415.
[3] A R Field et al., 29th EPS 2002 Conference, Montreux, P1.114.
[4] M Valovič et al., *Plasma Phys. Cont. Fus.* **44** (2002) A175.
[5] H Meyer et al., 29th EPS 2002 Conference, Montreux, P1.056.
[6] M. Greenwald, J. L. Terry, S. M. Wolfe, S. Ejima, M. G. Bell, S. M. Kaye, and G. H. Neilson, *Nucl. Fusion* **28** (1988) 2199.
[7] M.A. Mahdavi, et al., *(Proc. 18th IAEA Fusion Energy Conf., Sorrento, 2000),* paper IAEA-CN-77/EXP1/04, and M.A. Mahdavi, et al., *Nucl. Fusion* **42** (2002) 52.
[8] T.H. Osborne, et al. *Phys. Plasmas* **8** (2001) 2017.
[9] O.J.W.F. Kardaun for the International Confinement Database Working Group, *(Proc. 18th Fusion Energy Conf. Sorrento, 2000)*, paper IAEA-ITERP/04.
[10] O.J.W.F. Kardaun, *Report IPP-IR-2002/5-1.1*, Max-Planck-Institut für Plasmaphysik Garching (2002) http://www.ipp.mpg.de/ipp/netreports .
[11] P. N. Yushmanov, et al., *Nucl. Fus* **30** (1990) 1999.
[12] O. Kardaun and A. Kus for the L- and H-mode Database Group, *COMPSTAT XII, Physica Verlag, Heidelberg* **I** (1996) 313-319.